CHAPTER 5

Manifestation of exo-cyclic aromaticity in triangular heterocyclic B_2F_2X systems (X = O, S, Se, NH)

5.1.

INTRODUCTION

The idea of aromaticity is an age old concept[1-3] but its purpose and relevance is continually on the rise. Aromaticity can be considered as one of the most intriguing phenomena in chemistry which is evolving with time. The perception of aromaticity is associated with certain specific molecular characteristics such as added stabilization, planarity of the molecular systems, conjugation, electron delocalization[4-7] and most importantly a distinct reaction to applied magnetic field .[8-11] Presently, aromaticity is not the idea involving organic systems only but has incorporated all metal aromatic clusters[12-22] as well. Conjecture of aromaticity in planar π-electron systems by Huckel's (4n+2) rule [23] is one of best recognized and the most functional methods. In recent times, there has been an augmented interest in understanding and development of varied criteria for defining aromaticity.[24-26] Apart from the primary measures for defining aromaticity,[27-29] it has also been explained by electron density based indices.[30-34] Lately, aromaticity has become a significant tool in defining the stability and bonding in various chemical species surpassing the realm of organic chemistry[35-38] extending to inorganic moieties.[20-22] Also acyclic compounds have been found to have aromatic stability[39] thus implying that aromaticity can no longer be confined to the field of classical conjugated organic systems. In a recent theoretical work, it has been shown that exo-cyclic aromaticity is possible in planar systems; i.e., aromaticity is achieved through back-donation of electrons from thesubstituents.[40] The concept of 2p-2p orbital interaction or back-donation of fluorine has been well identified in the organic and inorganic domain.[41-43] Both the inductive effect and the resonance or the back-donation effect play a vital role when the non-bonded pair of electrons of fluorine interact with the vacant orbital of the boron atom to which it is attached. The tendency of back-donation by fluorine has been established to be greater than that of the other halogen atoms such as chlorine and bromine, where the order of back-donation is found to be F>Cl>>Br .[44] The degree of back-donation decreases with the increase in the atomic sizes of the halogens since the 2p-2p interaction is more favorable as compared to the interaction between 3p and 4p orbital of chlorine and bromine respectively with the vacant 2p orbital of boron due to mismatch in the size of the orbitals.

In this work, we theoretically propose novel heteroatomic systems where exo-cyclic aromaticity is observed which is achieved through back-donation of electrons from exo-

cyclic fluorine atoms. The systems studied are cyclic heteroatomic B_2F_2X (where X=O, S, Se, NH) molecules (Figure 5.1). In order to understand the bonding and the structural properties of these systems, a systematic theoretical study has been performed. The molecules are optimized at different levels of theory using various DFT and *ab*-initio methodologies involving coupled-cluster singles and doubles (CCSD). The stability of the molecules isvalidated by the absence of any imaginary frequency, Energy Decomposition Analysis (EDA)[45] computation of the Ring Strain Energy (RSE)[46] and higher HOMO-LUMO gaps.The aromaticity is analyzed and estimated through Nucleus Independent Chemical Shift (NICS),[47] Canonical Molecular Orbital NICS (CMO-NICS)[48] Multi Centre bond Index (MCI),[31] Adaptive Natural Density Partitioning (AdNDP)[49] and Aromatic Stabilization Energy (ASE).[50] As a whole, this work elucidates exo-cyclic aromaticity in novel systems with three-membered heteroatomic rings.

5.2.

COMPUTATIONAL DETAILS

Gaussian 09W suite of software was used for the minimum energy search and frequency calculationat various DFT (UB3LYP, UB3PW91, UPBEPBE, UBLYP and UCAM-B3LYP) and *ab-initio* (UCISD, UQCISD, UCCSD) methodologies using aug-cc-pvdz basis, T1 diagnostic run was carried out at UCCSD(t1diag)/aug-cc-pvdz level, computation of the HOMO-LUMO gap at ub3lyp/ aug-cc-pvdz level and NICS evaluation at various DFT levels (UB3LYP, UB3PW91, UPBEPBE, UBLYP and UCAM-B3LYP) with aug-cc-pvdz basis.[51] The Energy Decomposition Analysis at UB3LYP/aug–ATZP level and the CMO-NICS evaluation at LDA/DZ level are performed by the ADF program.[52] The Ring Strain Energy is calculated by the AIM version program[53] at UB3LYP/ aug-cc-pvdz level. The chemical bonding analysis employing the AdNDP orbitals are visualized and the multicentre bond aromaticity index (MCI) is calculated at UB3LYP/aug-cc-pvdz level using Multiwfn (A Multifunctional Wave function Analysis).[54] For the calculation of ASE, Gaussian 09W suite of software, Multiwfn and OpenMX 3.6 quantum chemistry code[55] are used.

5.3.

RESULTS AND DISCUSSION

5.3.1. Molecular Geometry

The optimized structures of the heteroatomic molecules B_2F_2X (where X=O, S, Se, NH) with their bond lengths in Å and B-X-B bond angles in degrees as computedin uccsd/ aug-cc-pvdz level of theory are given in Figure 5.1. The greater stability of the molecular systems can be accounted from the high minimum frequency value, the viability of the molecules are further substantiated by the absence of an imaginary frequency and the existence of allow ground state minimum energy as provided in Tables 5.1, 5.2, 5.3 and 5.4 for the B_2F_2O, B_2F_2S, B_2F_2Se and B_2F_2NH systems respectively. The structural reliability of the molecular systems is further established through Energy Decomposition Analysis (EDA) based on the approach of Ziegler and Rauk.[45] The individual atomic fragments are taken into consideration for the EDA. In this method the interaction energy (ΔE_{int}) is divided into three major components namely electrostatic interaction (ΔV_{elstat}), Pauli repulsive orbital interaction (ΔE_{pauli}) and attractive orbital interaction (ΔE_{orb}) as shown,

$$\Delta E_{int}=\Delta V_{elstat}+\Delta E_{pauli}+\Delta E_{orb} \qquad (5.1)$$

Here, the ΔV_{elstat} represents the classical electrostatic interaction between the fragments as they are brought together to form the final complex. ΔE_{pauli} corresponds to the repulsive interaction between the filled orbital, generally termed as steric interaction.[56]ΔE_{orb} corroborates the interactions between the occupied orbitals of one fragment to the unoccupied orbitals of the other fragment and also takes into account the interactions between the occupied and virtual orbitals of the same fragment.[45] The rationally high negative value of the total interaction energy as evident from Table 5.5 advocates towards the structural integrity of the molecular systems. Also a T1 diagnostic run from CCSD calculations have been performed to confirm the single-reference character of the molecules studied. The T1 diagnostics of species vary in the range of 0.015-0.017 as evident from Table 5.6 which are less than 0.02 thus advocating towards a single-reference character, as suggested by Lee and Taylor.[57]

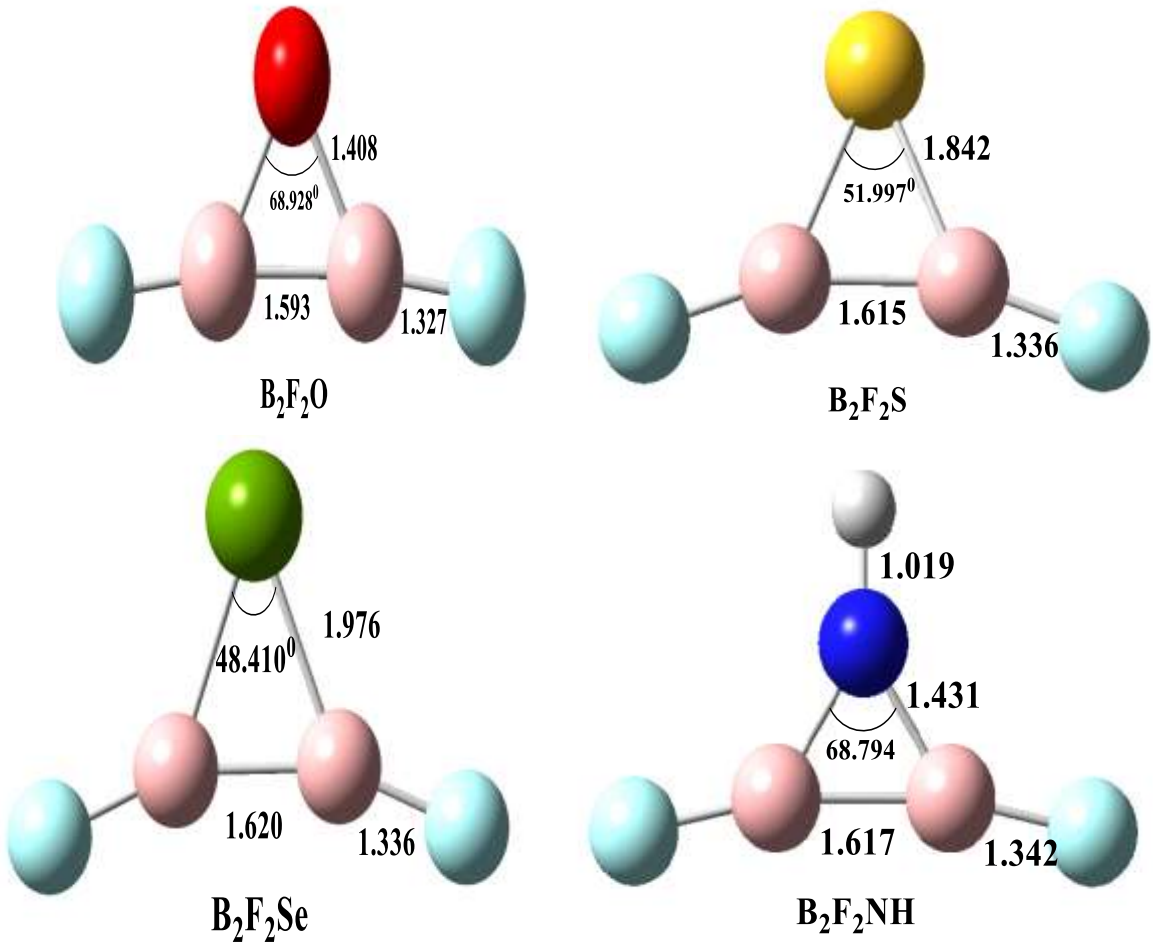

Figure 5.1. Optimized structure of B_2F_2O, B_2F_2S, B_2F_2Se andB_2F_2NH and their bond lengths in Å and the B-X-B bond angles in degree computed in uccsd/aug-cc-pvdz level, theboron, fluorine, oxygen, sulfur, selenium, nitrogen and hydrogen are represented by pink, cyan,red, yellow, green, blueand grey respectively.

Table 5.1. The optimized bond lengths (in Å), bond angles (in °), minimum energy (in a.u.) and minimum frequency (in cm^{-1}) of **B_2F_2O** at different unrestricted DFT and *ab initio* methodologies using aug-cc-pVDZ basis set.

Methodology (along with aug-cc-pvdz)	**B-B bond length(in Å)**	**B-O bond length(in Å)**	**B-F bond length (in Å)**	**< B-O-B (in °)**	**Minimum energy (in a. u.)**	**Minimum frequency(in cm^{-1})**
UCISD	1.58074	1.39251	1.31694	69.16405	-324.00	265.04
UQCISD	1.59440	1.41052	1.32888	68.82957	-324.03	251.94
UCCSD	1.59361	1.40804	1.32725	68.92894	-324.03	254.06
UB3LYP	1.57700	1.39737	1.31793	68.70360	-324.78	248.88
UB3PW91	1.57498	1.39795	1.31700	68.57105	-324.65	248.34
UPBEPBE	1.58413	1.41404	1.32735	68.13154	-324.44	236.47
UBLYP	1.58608	1.41416	1.32954	68.22043	-324.74	237.57
UCAM-B3LYP	1.57211	1.38981	1.31292	68.88600	-324.68	251.03

Table 5.2. The optimized bond lengths (in Å), bond angles (in °), minimum energy (in a.u.) and minimum frequency (in cm^{-1}) of **B_2F_2S** at different DFT and ab initio methodologies using aug-cc-pvdz basis set.

Methodology (along with aug-cc-pvdz)	**B-B bond length(in Å)**	**B-S bond length(in Å)**	**B-F bond length (in Å)**	**< B-S-B (in °)**	**Minimum energy (in a.u)**	**Minimum frequency(in cm^{-1})**
UQCISD	1.61734	1.84560	1.33699	51.97308	-646.63	241.64
UCISD	1.60843	1.82758	1.32538	52.21321	-645.91	252.90
UCCSD	1.61567	1.84290	1.33585	51.99715	-646.63	243.49
UB3LYP	1.59364	1.83892	1.32563	51.35543	-647.74	243.50
UB3PW91	1.59483	1.83306	1.32480	51.57293	-647.59	244.73
UPBEPBE	1.59972	1.84713	1.33504	51.31989	-647.29	236.01
UBLYP	1.59805	1.85851	1.33709	50.92596	-647.68	234.27
UCAM-B3LYP	1.59194	1.82346	1.32090	51.76370	-647.65	247.66

Table 5.3. The optimized bond lengths (in Å), bond angles (in °), minimum energy (in a.u.), and minimum frequency (in cm^{-1}) of **B_2F_2Se** at different DFT and ab initio methodologies using aug-cc-pvdz basis set.

Methodology (along with aug-cc-pvdz)	**B-B bond length(in Å)**	**B-Se bond length(in Å)**	**B-F bond length (in Å)**	**< B-Se-B (in °)**	**Minimum energy (in a.u)**	**Minimum frequency(in cm^{-1})**
UQCISD	1.62129	1.98007	1.33828	48.33459	-2648.91	209.72
UCISD	1.61343	1.96030	1.32573	48.60141	-2648.88	220.07
UCCSD	1.62062	1.97635	1.33655	48.41014	-2648.90	211.17
UB3LYP	1.59634	1.98015	1.32567	47.54242	-2651.08	211.00
UB3PW91	1.59822	1.97064	1.32488	47.84610	-2650.96	212.28
UPBEPBE	1.60132	1.98680	1.33552	47.53059	-2650.43	204.29
UBLYP	1.59910	2.00457	1.33731	47.01442	-2651.08	202.46
UCAM-B3LYP	1.59508	1.95938	1.32111	48.02534	-2651.09	215.41

Table 5.4. The optimized bond lengths (in Å), bond angles (in °), minimum energy (in a.u.) and minimum frequency (in cm^{-1}) of **B_2F_2NH** at different DFT and ab initio methodologies using aug-cc-pvdz basis set.

Methodology (along with aug-cc-pvdz)	**B-B bond length(in Å)**	**B-N bond length(in Å)**	**B-F bond length (in Å)**	**N-H bond length (in Å)**	**< B-N –B (in °)**	**Minimum energy (in A.U)**	**Minimum frequency(in cm^{-1})**
UQCISD	1.61776	1.43222	1.34415	1.01932	68.77968	-304.17	242.64
UCISD	1.60315	1.41842	1.33259	1.01000	68.83053	-303.42	258.39
UCCSD	1.61696	1.43126	1.34265	1.01920	68.79390	-304.17	244.52
UB3LYP	1.59937	1.41923	1.33276	1.01995	68.60454	-304.90	241.78
UB3PW91	1.59786	1.41908	1.33169	1.01886	68.52565	-304.77	242.67
UPBEPBE	1.60707	1.42993	1.34156	1.02902	68.38031	-304.56	229.42
UBLYP	1.61037	1.43073	1.34436	1.02984	68.49682	-304.84	230.59
UCAM-B3LYP	1.59287	1.41320	1.32822	1.01704	68.60613	-304.79	230.59

Table 5.5. Summary of energy decomposition parameters of B_2F_2O, B_2F_2S, B_2F_2Se and B_2F_2NH computed at ub3lyp/aug-cc-pVDZ level.

Molecules	**ΔE_{Pauli} (Kcal/mol)**	**ΔV_{elstat} (Kcal/mol)**	**ΔE_{orb} (Kcal/mol)**	**$\Delta E_{int}(=\Delta E_{Pauli}+\Delta V_{elstat}+\Delta E_{orb}$ (Kcal/mol)**
B_2F_2O	2954.85	-667.25	-2780.13	-492.53
B_2F_2S	2607.85	-612.66	-2419.45	-424.26
B_2F_2Se	2521.45	-602.87	-2380.41	-461.83
B_2F_2NH	3362.75	-717.70	-3265.88	-620.83

Table 5. 6. The T1 diagnostic values computed at the CCSD(t1diag)/aug-cc-pvdz level.

Molecules	**T1(diag)**
B_2F_2O	0.017
B_2F_2S	0.016
B_2F_2Se	0.015
B_2F_2NH	0.016

Evaluation of their structures reveals that these heteroatomic molecules display planar geometry thereby indicating the possibility of aromatic behavior in such systems since planarity of the system is a prerequisite for a molecule to be aromatic. We intuit that these molecules may have achieved the *aromatic sextet* as a consequence of back-donation of paired electrons from the substituent fluorine atoms to the vacant orbitals of the boron atoms as according to the scheme described in Figure 5.2 which agrees with Huckel's (4n+2) rule for aromaticity.

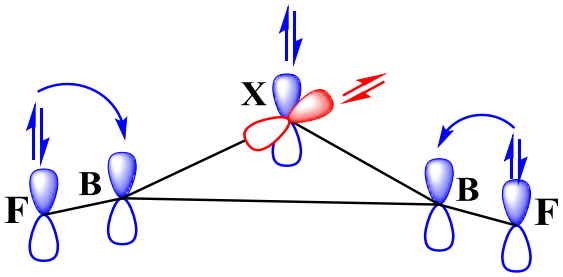

Figure 5.2. Orbital representation of the **B_2F_2X** molecules comprising of 6 π-electrons showing back donation of electrons from the fluorine atom to the vacant orbital of boron forming an aromatic π-cloud.

The B_2F_2X molecular systems possessing the group 16 heteroatom O, S and Se consisting of two lone pair of electrons occupying two orthogonal orbitals, so only one lone pair of electrons represented by blue pair of arrows are likely to be responsible for aromaticity which lies in plane with the plane of the vacant orbital of the boron atoms which are in turn being filled by back donating pair of electrons from the fluorine atoms as depicted in Figure 5.2. The other lone pair of electrons characterized by red pair of arrows of the heteroatom O, S, Se is not involved since it is orthogonal to the π aromatic plane. In B_2F_2X system consisting of the group 15 heteroatom N, two lone pair of electrons are present over the nitrogen atom. Two fluorine atoms donate two lone pairs, i.e., four electrons from fluorine atoms and two electrons are gained from the heteroatom thereby achieving the 6 π-electrons responsible for attaining aromaticity as in accordance to Huckel's(4n+2) rule.

5.3.2. Ring Strain Energy

The molecules studied are planar and cyclic three member rings which are similar to thecyclopropane moiety where ring strain is an important parameter for their stability, so here the ring strain is calculated with the aid of Bader's Quantum theory of Atoms in Molecules (QTAIM).[46] The Lagrange kinetic energy density value G (r) computed at the Ring Critical Point (RCP) can be used to evaluate the ring strain in these small rings, with the application of the Regression equation, RSE= {337.72 × G (r) – 8.115}.[58] The 'atoms in molecules'analysis is carried out by the AIM version program at ub3lyp/ aug-cc-pvdz level of theory. The computed values of the Ring Strain Energy in kcal/mol for our studied systems are given in Table 5.7.

Table 5.7. The Ring Strain Energy in kcal/mol computed at ub3lyp/ aug-cc-pvdz level.

Molecules	RSE (Kcal/mol)
B_2F_2O	29.22
B_2F_2S	21.20
B_2F_2Se	16.52
B_2F_2NH	28.49

The computed Ring Strain Energy values are in parity with the Ring Strain Energy values of experimentally observed stable three member cyclic systems[59-61] thereby indicating towards the structural stability and viability of the studied molecular systems. It also hints towards the presence of sigma aromaticity in the systems[62] which accounts for the reduced strain energy in the three-member planar rings. The stability of the three member planar cyclic ring structure encourages the prospect of circular electronic delocalization which is the genesis of aromaticity.

5.3.3. Molecular Orbital Analysis

The HOMO-LUMO gap can be considered as a direct measurement of kinetic stability[63-70] as a greater HOMO-LUMO gap would mean a higher kinetic stability. The molecules studied have a reasonably high HOMO-LUMO gap (Table 5.8) and since an appreciable HOMO-LUMO separation should be present for the molecules to be viable[71] thereby indicating that our systems are stable and also suggests of the closed shell nature of the molecules. This is a clear indication of the fact that these systems may have (4n+2) π aromatic electrons where all π-electrons are paired in bonding molecular orbitals.

Table 5.8. HOMO- LUMO gap in eV computed in ub3lyp/ aug-cc-pvdz methodology.

Molecules	HOMO-LUMO gap (eV)
B_2F_2O	4.43
B_2F_2S	6.637
B_2F_2Se	4.717
B_2F_2NH	6.593

The above analysis shows that these molecular three- member ring structures are reasonably stable thereby encouraging us to explore the possibility of circular electronic delocalization which direct towards aromaticity.

5.3.4. Aromaticity analysis employing NICS, CMO-NICS and MCI

Quantifying aromaticity is a challenge due to its multidimensional nature, [72-74] but the most efficient method of quantifying aromaticity is NICS, which was postulated by Schleyer and his co-workers.[47] The negative value of the absolute magnetic shielding gives the definition of NICS. A ghost atom is used for the determination of NICS through computational methodologies like GIAO.[75-78] In this work, the NICS values for the heterocyclic B_2F_2X systems are computed using UB3LYP, UB3PW91, UPBEPBE, UBLYP and UCAM-B3LYP methodology along with aug-cc-pvdz basis set which are represented in Table 5.9. The NICS values are computed by placing the ghost atom at the centre of the ring [NICS(0)] to account for the contribution of the σ-electrons to aromaticity and 1 Å above and below the plane i.e.,[NICS (1)] and [NICS(-1)] respectively to estimate the π-aromaticity of the systems. In harmony with NMR chemical shift principle, the NICS values are reported with negative signs. Positive NICS value signifies a paratropic magnetic field corresponding to antiaromatic systems whereas a negative NICS value signifies a diatropic magnetic field which correlates to aromatic systems.

The NICS (0) and NICS (1) computed for our systems are highly negative which indicates that the heterocyclic B_2F_2X systems are strongly aromatic. If we compare for the negative NICS (1) values, elements (O, S and Se) containing B_2F_2X systems than it is observed that thetrend is O<S<Se since the order of electronegativity is just the opposite so oxygen attracts the electrons more towards itself as compared to sulphur then selenium so the

order of electron delocalization is highest for Se, then S and then O. The NICS (1) value of nitrogen is also comparatively less owing to its higher electronegativity. The observation is in accordance to the notion that aromaticity increases with the decrease in the electronegativity difference between a heteroatom and its neighbouring atoms.[79]

Dissected Canonical Molecular Orbital NICS (CMO-NICS) analysis of B_2F_2O system is carried out to classify the orbitals contributing to σ and π aromaticity respectively. CMO-NICS calculations for B_2F_2O yield orbital contributions of −8.82 ppm from π, -17.422 ppm from valence σ towards the total of −26.242 ppm. From the orbital picture of the CMO contributing towards π-aromaticity {Figure 5.3(a)} it is apparent that the p_z orbitals of all the atoms including the exo-cyclic Flourine atoms are involved in formation of the π-cloud over the molecular plane.The orbital picture of the CMO contributing towards σ aromaticity {Figure 5.3(b)} reveals that the hybridized orbitals of the threeatoms i.e., the heteroatom and the two boron atoms are involved in the formation of this canonical molecular orbital. It is also to be noted that fluorine atoms do not contribute to the σ aromaticity at all. The picture becomes much clearer if we consider the population analysis provided in Table 5.10, where a 3-centred bond is present with the involvement of two sp^2 hybridised orbitals of boron and a pure in-plane p- orbital of the heteroatom (oxygen). So the σ aromaticity arises due to the delocalization of electrons across the trigonal ring through the planar heteroatom-bonds with the participation of two sp^2 hybridised orbitals of boron and an in-plane pure p-orbital of oxygen without the involvement of the flourine atoms. The trend of σ aromaticity is opposite to that of the trend followed by π aromaticity, it is highest for the heteroatom that are comparatively smaller in size, i.e., the systems containing the heteroatom oxygen and nitrogen have higher NICS (0) values implying higher σ aromaticity which is also supported by the CMO-NICS analysis. A shorter bond distance between the heteroatom (N and O) and the boron atom facilitates a greater in-plane delocalization thereby accounting for a higher σ aromaticity in B_2F_2O and B_2F_2NH systems. As the size of the heteroatom gradually increases down the group the bond distance between the heteroatom and the boron atom consequently increases as evident from Figure 5.1 thereby reducing the in-plane delocalization and correspondingly the σ aromaticity in B_2F_2S and B_2F_2Se systems. From the observation it is apparent that there exists an antagonistic relationship between σ and π aromaticity. This σ aromaticity accounts for the reduced strain energy in the three-member rings.[62]

Table 5.9. The nucleus-independent chemical shift (NICS) values in ppm at the plane of the ring (NICS (0)) and at 1 Å above the plane of the ring (NICS (1)) in different DFT methodologies using aug-cc-pVDZ basis set.

Molecules	**Methodology (along with aug-cc-pvdz)**	**NICS(0)**	**NICS(1)**
	UB3LYP	-25.8965	-9.3217
	UB3PW91	-25.4372	-9.3164
B_2F_2O	UPBEPBE	-24.9269	-9.3870
	UBLYP	-25.1485	-9.3241
	UCAM-B3LYP	-26.2475	-9.3766
	UB3LYP	-12.0535	-10.8361
	UB3PW91	-11.4657	-10.7858
B_2F_2S	UPBEPBE	-11.5345	-10.5561
	UBLYP	-12.0159	-10.5518
	UCAM-B3LYP	-12.1434	-11.0275
	UB3LYP	-10.0864	-11.2460
	UB3PW91	-9.5752	-11.1972
B_2F_2Se	UPBEPBE	-9.8592	-10.9167
	UBLYP	-10.2615	-10.8969
	UCAM-B3LYP	-9.9759	-11.4983
	UB3LYP	-23.7343	-8.5054
	UB3PW91	-23.4382	-8.4983
B_2F_2NH	UPBEPBE	-23.2253	-8.4073
	UBLYP	-30.1548	-9.1237
	UCAM-B3LYP	-23.7884	-8.5914

Table 5.10. Population analysis of the orbital which is responsible for σ aromaticity involving three centre bonds.

(Occupancy) Bond orbital/ Coefficients/ Hybrids

(1.98942) 3C*(1) B 1- B 2- O 3

(9.43%) 0.3070* B 1 s(32.75%)p 2.03(66.48%)d 0.02(0.76%)

-0.0003 0.5714 -0.0283 0.0166 0.0000

0.0000 -0.2477 -0.0716 -0.7690 0.0838

0.0000 0.0000 0.0547 -0.0199 0.0652

(9.43%) -0.3070* B 2 s(32.75%)p 2.03(66.48%)d 0.02(0.76%)

-0.0003 0.5714 -0.0283 0.0166 0.0000

0.0000 0.2477 0.0716 -0.7690 0.0838

0.0000 0.0000 -0.0547 -0.0199 0.0652

(81.15%) -0.9008* O 3 s(0.00%)p 1.00(98.94%)d 0.01(1.06%)

0.0000 0.0000 0.0000 0.0000 0.0000

0.0000 -0.9947 -0.0004 0.0000 0.0000

0.0000 0.0000 -0.1031 0.0000 0.0000

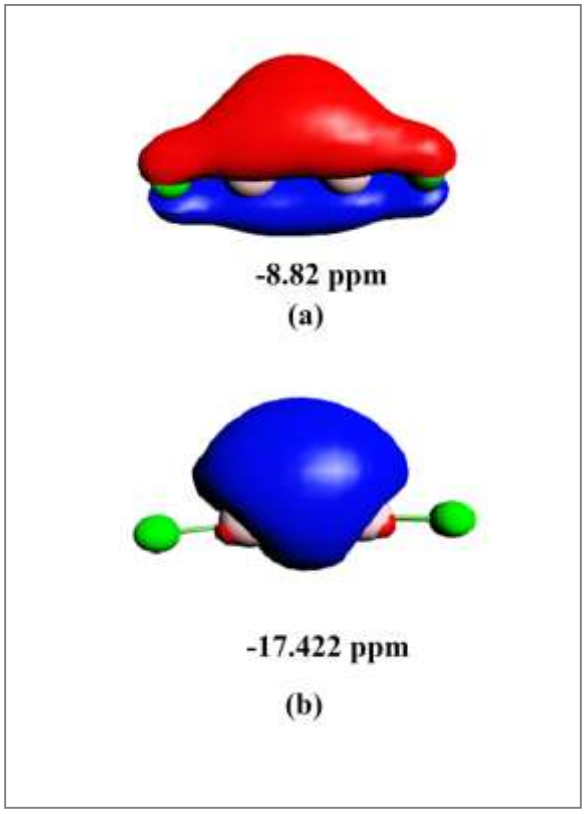

Figure 5.3. The CMOs with maximum diamagnetic contribution to π and σ aromaticity in (a) and (b)respectively, obtained through CMO-NICS analysis at the ring centre of the B_2F_2O molecule.

Apart from NICS, we also performed calculations using the Multiwfn program[54] to generate the multicentre bond aromaticity index (MCI). The MCI data for the studied molecular systems are provided in Table S6 of the Supplementary Information. The MCI values are in the range of 0.45-0.52 which strongly indicates the presence of aromaticity in these heterocyclic moieties.

5.3.5. Adaptive Natural Density Partitioning (*AdNDP) Analysis*

Adaptive Natural Density Partitioning is a theoretical analysis which provides a very proficient and an illustrative method to the understanding of the molecular orbital dependent wave functions. It is a recently developed method which was proposed in the year 2008 by Zubarev and Boldyrev[49] for determining chemical bonding patterns in general molecular systems. This method is based on the simple Lewis concept that describes the chemical bonding with respect to the electron pair thereby characterizing the electronic structures as n-centered-2 electron bonds where the value of n ranges from 1 to the total number of atoms present in the studied molecular systems. It figure outs the elements responsible for Lewis

bonding and also the elements responsible for delocalized bonding which can be correlated with the concepts of aromaticity and antiaromaticity. AdNDP is an overview of NBO analysis as was proposed by Weinhold[80,81] from a computational view point on the basis of the diagonalization of the blocks of the first order density matrix based on natural atomic orbitals. AdNDP bonding patterns are in consonance with the point group symmetry of the molecular systems and resonating structures are generally avoided. The main advantage of this method is that it effortlessly links the Canonical Molecular Orbitals (CMO) and the Natural Bonding Orbitals (NBO). AdNDP orbitals for our systems are investigated using Multiwfn (A Multifunctional Wave function Analysis program).[54]

The AdNDP analysis has been performed for all our systems as presented in Figure 5.4.The quest for the all-centre-2 electron bond whose natural occupation number ranges from 1.99-2.00|e| indicates a strong aromatic character in the studied systems. The visualization of the AdNDP orbitals reveals that the aromatic π cloud hovers over the molecular moiety comprising of the heteroatom (O, S, Se and N) along with the boron and the fluorine atom thereby indicating that the fluorine atoms are involved in aromaticity. This portrayal of the 5-centered 2-electron AdNDP orbital signifies the role of the substituent fluorine atoms in developing aromaticity thus strongly establishing our notion of exo-cyclic aromaticity in these systems (Figure 5.4).

B_2F_2O	 **B_2F_2O** Occupation No. 1.99
B_2F_2S	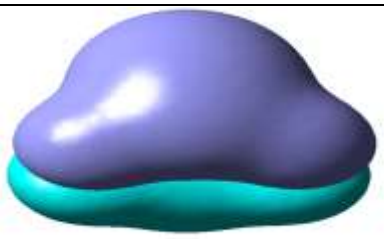 **B_2F_2S** Occupation No. 1.99
B_2F_2Se	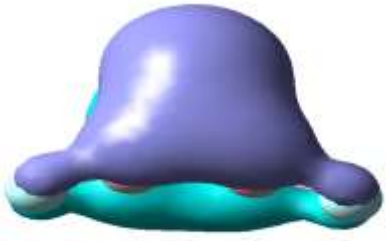 **B_2F_2Se** Occupation No. 1.99
B_2F_2NH	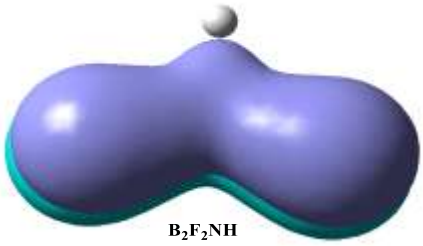 **B_2F_2NH** Occupation No. 2.00

Figure 5.4. The AdNDP orbitals of the studied systems from top view with their natural occupation numbers.

5.3.6. Aromatic Stabilization Energy(ASE)

In a recent work, aromaticity is quantified with respect to the energy stabilization due to circular π-electrons delocalization, termed as the Aromatic Stabilization Energy (ASE).[50] The expression for ASE for conventional benzene like systems was derived[54] to be

$$ASE = \sum_{i,j} \frac{t_{ij}^2}{U} \left(n_{i\sigma} n_{j\sigma'} + n_{i\sigma'} n_{j\sigma} \right) ELF^2 \quad (5.2)$$

Therefore, from Eq. (2), we can relate the π-electron delocalization energy (ASE) to the inter-site hopping integral (t_{ij}) and the onsite repulsion energy (U). The electronic population engaged in delocalization is obtained as a product of spin – orbital population ($n_{i\sigma}$ and $n_{j\sigma'}$) within the unrestricted framework and the degree of delocalization, which is estimated from electron localization function (ELF).

As already mentioned, the above equation is applicable for benzene like aromatic molecules, which are different from the studied system in terms of the electronic structure and aromaticity type.In the systems studied here, specifically the migration of the lone pair of electrons in between the boron and fluorine completes the loop of electronic circulation and thus makes the pattern of electron delocalization unique and different to conventional aromatic systems. To agree with this representation of electron delocalization, the above equation is divided into two components as

$$ASE = \sum_{B,X} \frac{2t_{ij}^2}{U} (n_{B\sigma} n_{X\sigma'} + n_{B\sigma'} n_{X\sigma}) ELF^2 + \sum_{F,B} \frac{2t_{ij}^2}{U} (n_{F\sigma} n_{B\sigma'} + n_{F\sigma'} n_{B\sigma}) ELF^2 \quad (5.3)$$

Here, the first part stands for the electron delocalization within B-X ring, it is multiplied by two to account for two lone pair of electrons of the heteroatom X and the second part quantifies stabilization for electron delocalization within Lewis acid-base pair. The probability of the lone-pair transfer from F to B is taken into consideration by multiplying by two.

TABLE 5.11. The Aromatic Stabilization Energy (ASE) of the studied molecular systems in kcal/mol.

MOLECULES	ASE(kcal/mol)
B_2F_2O	**17.1**
B_2F_2S	**22.8**
B_2F_2Se	**34.6**
B_2F_2NH	**21.1**

The high values of ASE as evident from Table 11 also advocate towards a significant stabilization of the molecules as a result of aromaticity. It can also be observed thatthe ASE values obtained are also in accordance and are in correlation to the NICS values. The values computed are comparable to highly stable classical aromatic systems[82, 83] thereby further accentuating the viability of these molecular systems. A method to localize Wannier function was given by Marzari and Vanderbilt named as Maximally Localized Wannier Function [MLWF] [84] which provides an enhanced bonding picture.

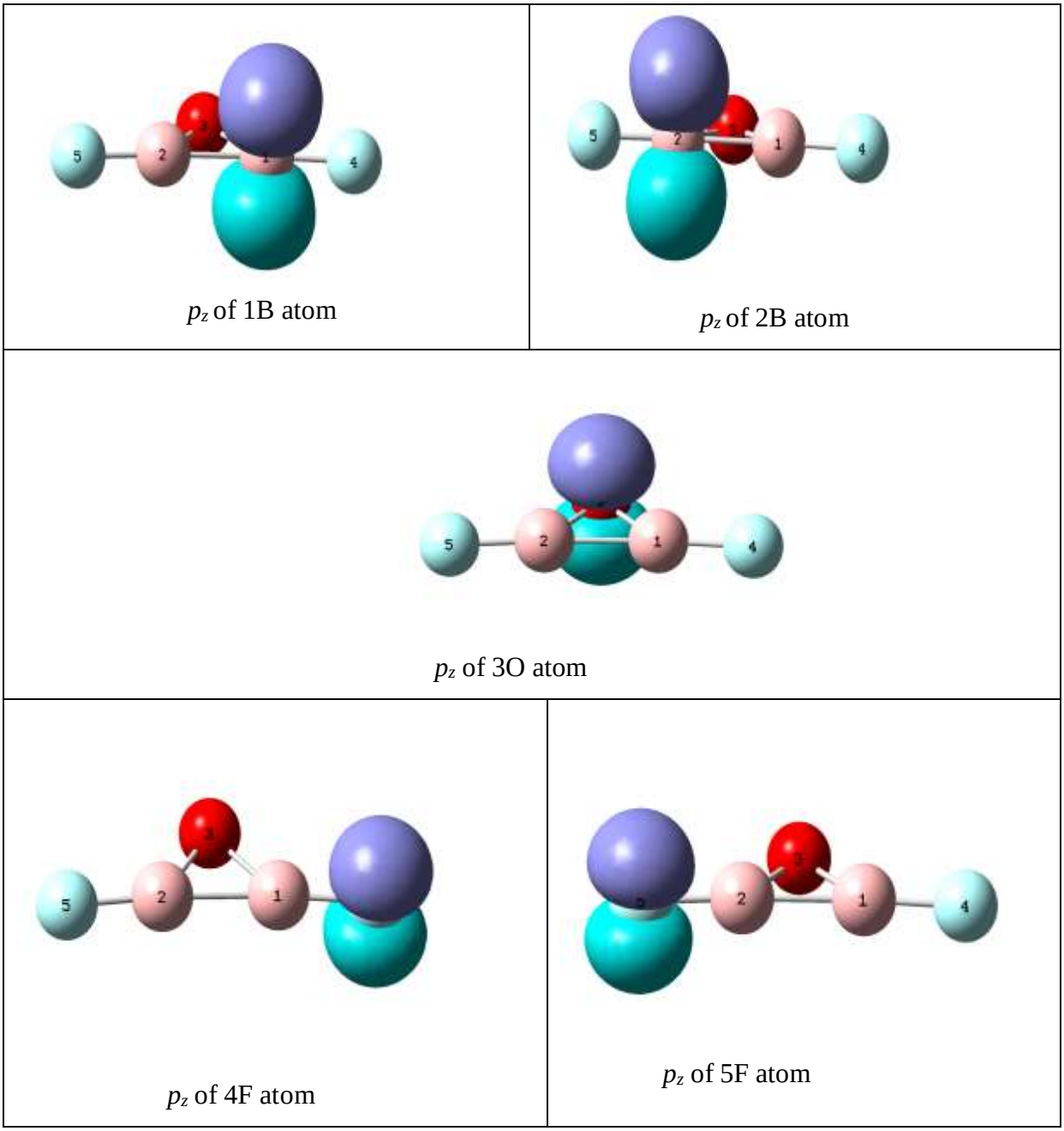

Figure 5.5. Maximally Localized Wannier Functions in B_2F_2O

The Maximally Localized Wannier Functions (MLWFs) obtained through OpenMX 3.6 quantum chemistry code[55] (Figure 5.5) provide a vivid picture that the p_z orbitals perpendicular to the molecular plane of all the atoms including the exo-cyclic atoms are involved in aromaticity as in accordance to our scheme described in Fig.2. thereby establishing our notion of exo-cyclic aromaticity where aromaticity is achieved through back donation of electrons of the fluorine atoms to the electron-deficient p_z orbitals of the boron atoms.

5.4.

CONCLUSIONS

The observation of unique aromaticity obtained through back donation of 4π-electrons from substituent exo-cyclic flourineatoms to the vacantp_z orbitals of the boron atomsmake the study of these proposed novel three-membered heterocyclic planar systems an interesting addition to the domain of aromaticity. Rigorous computational study involving DFT and *ab initio* calculations along with Energy Decomposition Analysis (EDA), the evaluation of Ring Strain Energy and HOMO-LUMO gap indicate towards the viability of the systems. The aromaticity of the molecule is evaluated through some standard criteria, specifically Nucleus Independent Chemical Shift (NICS) and Multi Centre bond Index (MCI). The dissected NICS analysis (CMO-NICS) presents a clear picture of the molecular orbitals contributing towards σ and π aromaticity respectively. A coherent picture of the exo-cyclic nature of the aromatic π-cloud is viewed with the AdNDP analysis. The Aromatic Stabilization Energy (ASE) based on a fully *ab initio* approach is also reported which renders the proposed heterocyclic molecules to be remarkable 6 π -aromatic systems where the *magic number* is attained through an 'exo-cyclic' conjugation. These proposed molecules are unique and distinctive due to the presence of both the σ and the π aromaticity and the antagonistic relationship existing between them makes the systems aremarkable addition to the class of aromatic molecules and provide a significant scope of future study. The high stability of the molecular systems as apparent from the various computational analysis makes us hopeful regarding the investigational reality of these molecules.

5.5.

REFERENCES

1. Faraday, M. *M.Phil.Trans.Roy.London* **1825**, *115*, 440.
2. Kekulé, A. .*Bull.Soc.Chim.Paris* **1865**, *3*, 98.
3. Kekulé, A. *Ann.Chem.Pharm* **1866**, *137*, 129.
4. Garratt, P. J. *Aromaticity*; John Wiley & Sons, 1986.
5. Minkin, V. I.; Glukhotsev, M. N.; Simkin, B. Y. *Aromaticity and antiaromaticity: electronic and structural aspects;* John Wiley & Sons, Inc., New York, **1994**.
6. Bickelhaupt, F.; de Wolf, W. H. *Recl. Trav. Chim. Pays-Bas.* **1988**, *107*, 459

7. Kraakman, P. A.; Valk, J. M.; Niederla¨nder, H. A. G.; Brouwer, D. B. E.; Bickelhaupt, F. M.; de Wolf, W. H.; Bickelhaupt, F.; Stam, C. H. *J. Am. Chem. Soc.***1990**, *112*, 6638.
8. Schleyer, P. V. R.; Jiao, H. *J. Pure Appl. Chem.* **1996**, *68*, 209.
9. Schleyer, P. V. R.; Jiao, H.; Hommes, N. J. R. v. E.; Malkin, V.G.; Malkina, O. L. *J. Am. Chem. Soc.***1997**,*119*, 12669.
10. Poranne, G.P.; Stranger, A. *Magnetic and structural aspects*; Wiley: New York, **1994**.
11. Homray, M.; Misra, A.; Chattaraj, P. K. *Curr. Org. Chem.***2017**, *21*, 2699.
12. Katritzky, A. R. *Chem. Rev.* **2004**, *104*, 2125.
13. Aihara, J. I. *Pure Appl. Chem*. **1982**, *54*, 1115.
14. Graovac, A.; Trinajstic, N.International symposiumon aromaticity, Dubrovnik, 1979.
15. Nyulaszi, L. *Chem. Rev.* **2001**, *101*, 1229.
16. Minkin, V. I.; Minyaev, R. M. *Chem. Rev.***2001**, *101*, 1247.
17. Katritzky, A. R.; Jug, K.; Oniciu, D. C. *Chem. Rev.***2001**, *101*, 1421.
18. Li,X.; Kuznetsov, A.; Zhang, H.; Boldyrev, A. I.; Wang, L. *Science,***2001**, 291, 859.
19. Kuznetsov, A. E.; Birch, K. A.; Boldyrev, A. I.; Li, X.; Zhai, H.; Wang, L. *Science*, **2003**, *300*, 622.
20. Boldyrev, A. I.; Wang, L .*Chem. Rev.* **2005**, *105*, 3716.
21. Paul, S.; Misra, A. *Inorg Chem* **2011,** *50*, 3234.
22. Chattaraj, P. K.; Roy, D. R.; Duley, S. *Chem.Phys.Lett.* 2008, *460*,382.
23. Huckel,E. *Z. Phys*. **1931**, *70*, 204.
24. Hehre, W. J.; Radom,L.; Schleyer,P. v. R.; Pople, J. A. *Ab Initio molecular orbital theory*; Wiley, New York, 1986.
25. Xie, Y.; Schaefer III, H. F.; Thrasher, J. S. *J. Mol. Struct. Theochem.*, **1991**, *234*, 247.
26. Shaik, S.; Shurki, A.; Danovich, D.; Hiberty, P. C. *J. Mol. Struct.Theochem* **1997**, *398*, 155.
27. Krygowski, T. M.; Cyraski, M. K., *Chem. Rev.* **2001**, ***101***, 1385.
28. Poater, J.; Duran, M.; Solà, M.; Silvi, B. *Chem. Rev.* **2005**, *105*, 3911.
29. Cyraski, M. K. *Chem. Rev.* **2005**, *105*, 3773.
30. Matito, E.; Duran, M.; Solà, M. *J. Chem. Phys.* **2005**, *122*, 014109.
31. Bultinck, P.; Ponec, R.; Van Damme,S. *J. Phys.Org. Chem*. **2005**, *18*, 706.
32. Feixas, F.; Matito, E.;Poater, J.;Solà, M. On the performance of some aromaticity indices: A critical assessment using a test set. *J. Comput. Chem.* 2008, 29, 1543-1554.
33. Roy, D. R.; Bultinck, P.; Subramanium, V.; P. K. Chattaraj, J. Mol. Struc., **2008**, *854*, 35.
34. Feixas, F.; Matito, E.; Poater, J.; Solà, M. *Chem. Soc. Rev*. **2015**, *44*, 6434.
35. Misra, A.; Klein, D. J.; Morikawa,T. J. Phys. Chem. A **2009***, 113*, 1151.
36. Clar, E. *The Aromatic Sextet*; Wiley & Sons: New York, **1970**.
37. Misra, A.; Schmalz, T. G.; Klein, D. J. *J.Chem. Inf.Model*, **2009**, *49*, 2670.
38. Bhattacharya, D.; Panda, A.; Misra, A.; Klein, D. J. *J. Phys. Chem. A*, **2014**, *118*, 4325.
39. Gund, P. *J. Chem. Educ.* **1972**, *49*, 100.
40. Goswami, T.; Homray, M.; Paul, S.;Bhattacharya, D.; Misra, A. *Phys. Chem. Chem. Phys.* **2017**, *19*, 11744.
41. Gutowsky, H. S.; McCall, D. W. *J. Phys. Chem.* **1953**, *21*, 279.

42. Onak, T. P.; Landesman, H.; Williams, R. E.; Shapiro, I. paper presented to the Division of Inorganic Chemistry, 135th NationalMeeting of the American Chemical Society, Boston, Mass., April **1959**.
43. Cotton, F. A.; Wilkinson,G. *"Advanced Inorganic Chemistry,"*Interscience, London, **1966**, 256.
44. Olah, G. A.; Mo, Y. K.; Halpern, Y. *J Am Chem Soc* **1972**, *94*, 3551.
45. Ziegler, T.; Rauk, A. 1**977**, *46*, 1.
46. Bader, R. F. W. *Atoms in Molecules: A Quantum Theory;* Oxford University Press, Oxford, UK, **1990**.
47. Schleyer, P. v. R.;Maerke, C.; Dransfeld, A.; Jiao, H.; Hommes, N. J. R. v. E. *J Am Chem Soc*, **1996**, *118*, 6317.
48. Heine, T.; Schleyer, P. v. R.; Corminboeuf, C.; Seifert, G.; Reviakine, R.; Weber, J. *J. Phys. Chem. A* **2003**, *107*, 6470.
49. Zubarev, D. Yu.; Boldyrev, A. I. *Phys. Chem. Chem. Phys*. **2008**, *10*, 5207.
50. Paul,S.; Goswami, T.; Misra, A. *AIP Advances*, **2015**, *5*, 107211.
51. Gaussian 09, Revision B.01, Frisch, M. J.; Trucks, G. W.; Schlegel, H. B.; Scuseria, G. E.; Robb, M. A.; Cheeseman, J. R.; Scalmani, G.; Barone, V.; Petersson, G. A.; Nakatsuji, H.; Li, X.; Caricato, M.; Marenich, A. V.; Bloino, J.; Janesko, B. G.; Gomperts, R.; Mennucci, B.; Hratchian, H. P.; Ortiz, J. V.; Izmaylov, A. F.; Sonnenberg, J. L.; Williams-Young, D.; Ding, F.; Lipparini, F.; Egidi, F.; Goings, J.; Peng, B.; Petrone, A.; Henderson, T.; Ranasinghe, D.; Zakrzewski, V. G.; Gao, J.; Rega, N.; Zheng, G.; Liang, W.; Hada, M.; Ehara, M.; Toyota, K.; Fukuda, R.; Hasegawa, J.; Ishida, M.; Nakajima, T.; Honda, Y.; Kitao, O.; Nakai, H.; Vreven, T.; Throssell, K.; Montgomery, J. A., Jr.; Peralta, J. E.; Ogliaro, F.; Bearpark, M. J.; Heyd, J. J.; Brothers, E. N.; Kudin, K. N.; Staroverov, V. N.; Keith, T. A.; Kobayashi, R.; Normand, J.; Raghavachari, K.; Rendell, A. P.; Burant, J. C.; Iyengar, S. S.; Tomasi, J.; Cossi, M.; Millam, J. M.; Klene, M.; Adamo, C.; Cammi, R.; Ochterski, J. W.; Martin, R. L.; Morokuma, K.; Farkas, O.; Foresman, J. B.; Fox, D. J. Gaussian, Inc., Wallingford CT, 2009.
52. Amsterdam Density Functional (Theoretical Chemistry, Vrije Universitiet, Amsterdam, The Netherlands, http://www.scm.com).
53. AIMAll (Version 17.01.25), Todd A. Keith, TK Gristmill Software, Overland Park KS, USA, 2017
54. Lu, T.; Chen, F. Multiwfn: A multifunctional wavefunction analyzer*J. Comp. Chem*.**2012**, 33, 580-592.
55. The DFT code, OPENMX, is available at http://www.openmx-square.org under the GNU General Public License.
56. Pinter, B.; Fievez, T.; Bickelhaupt, F. M.; Geerlings, P.; F. DeProft, *Chem. Chem. Phys.***2012**, *14*, 9846.
57. Lee, J. T.; Taylor, P. R. *Int. J. Quantum Chem.***1989**, *36*, 199.
58. Bauzá, A.; Quiñonero, D.; Deyà, P. M.; Frontera, A. *Chem. Phys. Lett*., **2012**, *536*, 165.
59. Cox, J. D.; Pilcher, G.; *Thermochemistry of organic and Organometallic compounds;* Academic: London, 1970.
60. Benson, S. W. *Thermochemical Kinetics;* Wiley: New York, 1976.
61. Inagaki, S.; Ishitani, Y.; Kakefu, T. *J. Am. Chem. Soc.* **1994**, *116*, 13.

62. Dewar, M. J. S. *J. Am. Chem. Soc.* **1984**, *106*, 669.
63. Aihara, J. *J. Phys. Chem. A* **1999**, *103*, 7487.
64. Aihara, J. *Theor. Chem. Acc.***1999**, *102*, 134.
65. Aihara, J. *Phys. Chem. Chem. Phys.* **1999**, *1*, 227.
66. Parr, R. G.; Zhou, Z.; *Acc. Chem. Res*. **1993**, *26*, 256.
67. Liu, X.; Schmalz, T. G.; Klien, D. J. *Chem. Phys. Lett.* **1992**, *188*, 550.
68. Haddon, R. C.; Fukunaga, T. *Tetrahedron Lett.* **1980**, *21*, 1191.
69. Pearson, R. G. *Hard and soft acids and bases*; Dowden, Hutchinson and Ross: Stroudsburg, PA, 1973.
70. Manolopoulos, D. E.; May, J. C.; Down, S. *Chem. Phys. Lett.***1991**, *181*, 105.
71. Hoffmann, R.; Schleyer, P. V. R.; Schaefer, H. F. *Angew. Chem., Int. Ed.* **2008**, *47*, 7164.
72. Katrizky, A.; Barczymski, P.; Musumarra, G.; Pisano, D.; Szafran, M. *J. Am. Chem. Soc* **1989**, *111*, 7.
73. Schleyer, P. V. R.; Manoharan, M.; Jiao, H.; Stahl, F. *Org Lett.* **2001**, *3*, 3643.
74. Chen, Z.; Wannere, C. S.; Corminboeuf, C.; Puchta, R.; Schleyer, P. V. R. *Chem Rev.* **2005**, *105*, 3842.
75. London, F. *J. Phys. Radium.* **1937**, *8*, 397.
76. Cheeseman, J. R.; Trucks, G. W.; Keith, T. A.; Frisch, M. J. *J. Chem. Phys.* **1996**, *104*, 5497.
77. Schreckenbach, G.; Ziegler,T.; *J. Phys. Chem*. 1995, *99*, 606.
78. Schreckenbach, G.; Ziegler,T.; *Theor. Chem. Acc.*1998, *99*, 71.
79. Simkin, B. Y.; Minkin, V.I.; Glukhotsev, M.N. *Adv. Heterocyclic Chem*.**1993**, *56*, 304.
80. Foster, J. P.; Weinhold, F. *J. Am. Chem. Soc*. **1980**, *102*, 7211.
81. Reed, A. E.; Curtiss, L. A.;Weinhold, F. *Chem. Rev.***1988**, *88*, 899.
82. Katrizky, A.; Barczymski, P.; Musumarra, G.; Pisano, D.; Szafran, M. *J. Am. Chem. Soc* **1984**, *111*, 7.
83. Radhakrishnan, S.; Anathakrishnan, S. J.; Somanathan, N. *Bull. Mater. Sci.* **2011**, *34*, 713.
84. Marzari, N.;Vanderbilt, D. *Phys. Rev. B* **1997**, *56(20)*, 12847.